BOLLETTINO DI GEOFISICA TEORICA ED APPLICATA VOL. 43, N. 1-2, PP. 101-108; MAR.-JUN. 2002

Temporal evolution of large esplosive eruptions

S. DE ANGELIS[1, 2], C. VIGNOLA[1], R. SCANDONE[1] and L. GIACOMELLI[1]

[1] *Dipartimento di Fisica, Università degli Studi "ROMA TRE", Italy*
[2] *Dipartimento di Fisica, Sezione di Geofisica, Università di Bologna, Italy*

(Received June 19, 2001; accepted December 4, 2001)

Abstract - We propose a simple physical model for the temporal evolution of large explosive volcanic eruptions, based on the sudden decompression of a magma reservoir at shallow depth. The magma is water-saturated and the sudden decompression results in vesiculation that drives it out of the chamber. The viscoelastic response of the magma chamber walls plays an important role in controlling the style of the eruption. A temporal increase in the magma discharge rate is predicted when relaxation times are longer than 10^5s. The eruption ends when the chamber becomes sufficiently underpressured and collapses. We investigate the influence of the magma chamber geometry on the eruptive dynamics and the role played by the initial decompression and the gas bubble density. We are able to correctly reproduce the pattern of magma discharge rate and the duration of the May 18, 1980 eruption of Mt. St. Helens (Washington, U.S.A.).

1. Introduction

Large explosive eruptions are mainly characterized by a magma discharge increasing with time, later followed by a waning activity phase. The data collected during the three major explosive eruptions of the latest years (Mt. St. Helens 1980, El Chichon 1982, Mt. Pinatubo 1991) highlight the recurrence of three main features: a) a high volatile content of the magma, b) a magma discharge increasing with time, c) occurrence of deep seismicity (10-15 km) underneath the volcanic edifice at the end of the eruption, probably signalling the collapse of the magma chamber.

Wilson et al. (1980) suggest that the style of an eruption is mostly controlled by the geometry of the conduit and the physical properties of the magma. Woods (1995) and Vergniolle (1996) improved this model considering multiphase flow effects; the magma discharge rate variations are mainly controlled by the magma volatile content. Wilson et al.

Corresponding author: S. De Angelis, Dipartimento di Fisica, Università degli Studi "ROMA TRE", Via della Vasca Navale, 84, 00146 Roma, Italy; phone: +39 0655177301; fax: +39 065579303; e-mail: deangelis@neve.fis.uniroma3.it

(1980) and Carey et al. (1990) explain increasing magma discharge rate as consequence of the erosion and widening of the conduit. Over the last few years, Scandone (1996), Scandone and Giacomelli (2001), Bower and Woods (1997), Folch and Martì (1998) have suggested that the temporal evolution of explosive eruptions is controlled by the rheological behaviour of the magma chamber and by diffusive growth of bubbles in a gas saturated magma when decompressed. According to the model proposed by Scandone and Giacomelli (2001), explosive eruptions are driven by the growth of gas bubbles by diffusion of water from the melt. In this paper, we further develop this model by considering a magma chamber of finite dimensions, enclosed in a pseudo-rigid rock and connected to the surface by a conduit; the conduit geometry is considered variable during the eruption.

2. The model

We consider a cylindrical magma chamber enclosed in a country rock that behaves as a rigid body on the time scale of the eruption (Scandone and Giacomelli, 2001). The magma is water saturated. The pressure in the magma chamber $P(z)$ is the sum of a constant lithostatic term and a variable magmastatic contribution function of the depth z:

$$P(z) = \rho_{rock} \cdot g \cdot H_{top} + \rho_m \cdot g \cdot (z - H_{top}) \tag{1}$$

where H_{top} is the depth of the upper surface of the reservoir, ρ_m and ρ_{rock} are the mean densities of the magma inside the chamber and of the sorrounding rocks and g is the gravity acceleration. The saturation content of water in the magma is given by Henry's solubility law:

$$x(z) = n_0 \cdot \sqrt[k]{P(z)} \tag{2}$$

where k varies depending on the dissolved volatile species ($k = 2$ for H_2O). When the magma chamber is instantaneously decompressed, the volatiles exsolve and expand, leading to nucleation and diffusive growth of gas bubbles. On the basis of the analytical asymptotic model of Navon and Lyakhovsky (1998), the radial growth of the bubbles is given by:

$$R(t, z) = \left[\frac{2 \cdot D \cdot \rho_m \cdot (x_0(z) - x_f(z))}{\rho_g(z)} \cdot t - \frac{2}{3} \frac{D \cdot \eta}{P_f(z)} \frac{\rho_m}{\rho_g(z)} (2x_0 + x_f) \cdot \log\left(\frac{\Delta P}{\eta} \cdot t \right) \right]^{\frac{1}{2}} \tag{3}$$

where D is the diffusion coefficient, η is the mean viscosity of the melt, ΔP is the pressure difference between the bubbles and the surrounding melt, x_0 and x_f are the initial and final concentration of water, ρ_m and ρ_g the mean densities of the melt and of the gas, P_f the final pressure. The growing bubbles attain a final radius R_f in the time t_f.

The bubbles' growth causes an increase in volume of the magma-gas mixture and its emission out of the chamber. The velocity of growth of the bubbles strongly controls the magma flow rate. The volumetric increase of the magma-gas mixture as function of time will be (for spherical bubbles):

$$V(t) = \frac{4}{3} \cdot \pi \cdot N_d \cdot \int_{H_{base}}^{H_{top}} A \cdot R(t,z)^3 \cdot dz \tag{4}$$

where $A = \pi \cdot r^2$ is the cross sectional area of the chamber. The volumetric discharge rate will be simply given by the time derivative of the $V(t)$ function:

$$Q(t) = \frac{d}{dt} V(t) \tag{5}$$

The time-dependent density of the magma-gas mixture can be obtained by a simple mass conservation equation:

$$\rho_m V_{cham} = \rho(t) \cdot (V_{cham} + V(t)) \Rightarrow$$
$$\Rightarrow \rho(t) = \frac{V_{cham}}{V_{cham} + V(t)} \rho_m \tag{6}$$

3. Results

We analyze the influence of volume and depth of the magma chamber, the number density of bubbles and the decompression of the system on the temporal evolution of the eruption.

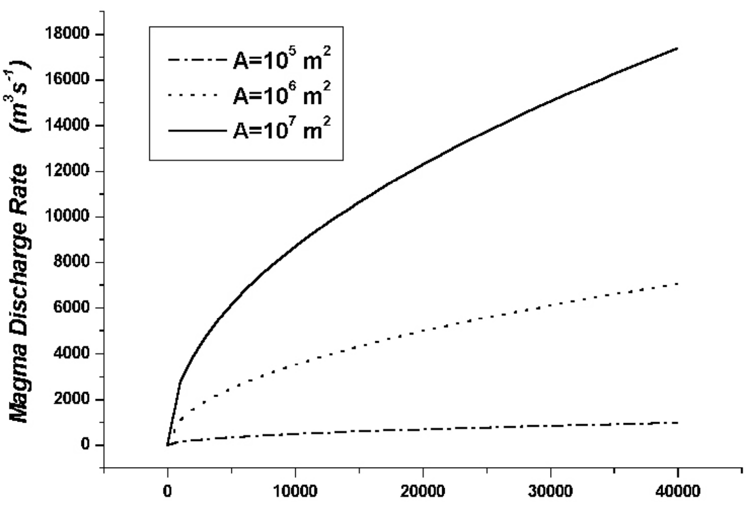

Fig. 1 - Magma Discharge Rate for different aspect ratio of the chamber. The volume of the reservoir is 10^{10} m^3 . The top surface of the chamber is at depth 6 km. The vertical extent and the cross-sectional area for the plotted curves are 10^5 m and 10^5 m^2; 10^4 m and 10^6 m^2; 10^4 m and 10^7 m^2.

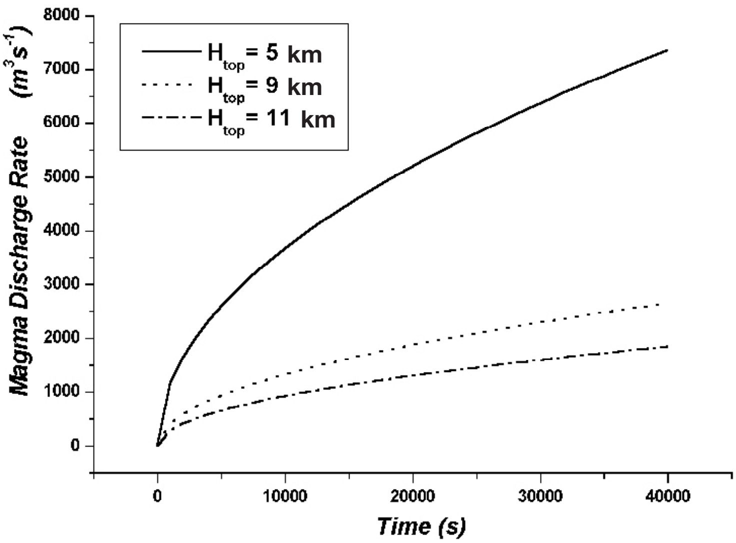

Fig. 2 - Variations of the discharge rate with time. The volume of the chamber is 10^{10} m^3 with a 10 km vertical extent; the depth of the upper surface of the chamber is 5 km, 9 km and 11 km for the plotted curves.

Fig. 1 shows the influence of aspect ratio of the magma chamber on the volumetric eruption rate. We consider chambers with a fixed volume of 10 km^3, at depth 6 km with different cross-sectional areas. The system is decompressed by 15 MPa.

Fig. 2 shows the influence of the depth of the chamber on the magma discharge rate; the different curves are for a volume of 10 km^3, a vertical extent of 10 km and depth of 5,9,11 km for the top surface of the reservoir.

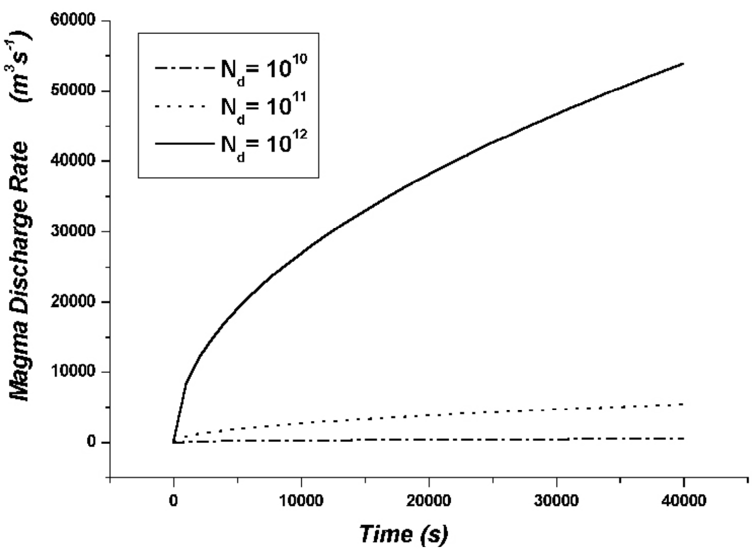

Fig. 3 - Magma Discharge Rate for different number densities of bubbles. The chamber volume is 10^{10} m^3, with vertical extent 10 km and the upper surface to a depth of 6 km. The curves show different patterns of the discharge rate for N_d=10^{10}, 10^{11} and 10^{12} m^{-3}.

In Fig. 3 we investigate, for a fixed geometry, the influence of different values of the bubble number density on the eruption rate. We consider a 10 km^3 chamber, at depth 6 km, with vertical extent 10 km. The system is decompressed by 15 MPa. The three curves illustrate the volumetric eruption rate for values of N_d 10^{10}, 10^{11} and 10^{12} m^3.

4. Discussion

The model in this paper provides an important insight into the analysis of the temporal evolution of large explosive volcanic eruptions. Previous time-dependent models were based on the hypothesis of an elastic behaviour of the magma chamber walls. In our model, we consider a pseudo-rigid response of the wall rocks with relaxation times longer than the eruption duration. The typical time of an explosive eruption is strictly related to the growth velocity of gas bubbles by diffusion from the melt (i.e. their growth time). Number densities $10^{10} \leq N_d \leq 10^{12}$ result in growth times $10^4 \leq t_f \leq 10^5$ s. Since typical values for the relaxation times of the wall rocks are of the order of 10^6, to a good approximation, we can model the magma chamber as a rigid envelope. We suggest that the mechanical behaviour of the rocks sorrounding the magma chamber controls the mechanism of the eruption. An elastic response of the chamber walls produces a high pressure gradient between the chamber and the surface (the stress applied to the chamber walls in this case closely approached the lithostatic load) during the first stages of the eruption and a following gradual decrease of the overpressure that does not permit significant vesiculation; this is typical for long-lasting (days to months) effusive eruptions. On the other hand, in the case of a pseudo-rigid behaviour of the chamber walls (that do not accommodate the pressure variations of the magma-gas mixture), the expansion of a volatile phase drives the magma out of the chamber; this is typical for short-lasting (hours to days) explosive eruptions.

Our simulation produces temporally increasing magma discharge; the rate of increase is controlled by the geometry of the chamber, the number density of bubbles and the initial decompression of the system. We observe the following three main facts.

1. For a given volume, and in a fixed time period, shallow chambers of large cross-sectional areas produce much larger eruptions than deep reservoirs of small cross-sectional areas (Fig. 1). Chambers of large aspect ratio tend to erupt with a higher discharge rate since the magma is located at shallow depths where most of the volatiles are easily exsolved because of the low value of the lithostatic pressure.
2. The discharge rate is sensitive to the chamber depth; deeper chambers produce slower increase in the eruption rate. In the deeper chambers, the lithostatic pressure is greater and it takes longer for the volatiles to exsolve (Fig. 2).
3. For a given chamber geometry and initial decompression, variations in the number density of bubbles can lead to significant changes in the eruption rate. Larger number densities result in a faster increase in the discharge rate (Fig. 3). Values of $N_d > 10^{11}$ - 10^{12} m^{-3} cause a fast growth of the bubbles that result in a large volumetric increase with time. Values

of $N_d < 10^{11}$ - 10^{12} m^{-3} cause a slower growth of the gas bubbles and a smaller volumetric increase with time.

We noted that the eruption ends when the chamber is sufficiently underpressured and the wall rocks fail, sealing the reservoir and turning back to the original pressure conditions. The failure of the rocks depends on local factors as the regional stress field and on the depth and geometry of the magma chamber. In chambers of large aspect ratio it is not unusual that underpressuring leads to caldera formation.

5. Simulation of the May 18, 1980 event at Mt. St. Helens (Washington, U.S.A.)

On May 18, 1980, at 08:32 a.m. P.D.T., a magnitude 5 earthquake at Mt. St. Helens triggered a huge landslide of the north flank of the volcano. The landslide caused a decompression of the hydrothermal system and resulted in a lateral blast that devasted a 650 km^2 area. About 30 minutes after the blast, debris falling from the unstable crater and lasser vesiculating dacitic magma were explosively ejected in a dark coloured eruption column that ranged from 14 to 16 km in height above the volcano. The eruption column lightened in colour and became more energetic at about noon as a supply of gas-rich magma was reaching the surface; pumiceous pyroclastic flows were later observed northward from the crater. After the pyroclastic flow phase a 19 km high Plinian column was again observed. The eruptive activity began to decline in the late afternoon (at about 5:30 p.m.) and ended during the night.

In the simulation of the eruption, we consider a cylindrical magma chamber at a depth of 6 km, and a cross-sectional area of 10^7 m^2 with a total volume of the deep feeding system estimated in 10^{10} m^3. The system is suddenly decompressed by an amount of 20 MPa because of the failure of the north flank of the volcano. We use a diffusion coefficient $D = 10^{-12}$ m^{-2} s^{-1} and a bubble number density $N^d = 10^{11}$ m^{-3} based on experimental data (Navon and Lyakhovsky, 1998).

We obtain from the model a magma discharge rate increasing with time and a total duration of the eruption of 10.5 hours compared with the observed 9 hours duration (Christiansen and Peterson, 1981). The magma discharge rate was experimentally estimated by a technique that makes use of the height of the eruption column (Harris et al., 1981). The relationship between the magma discharge rate Q and the column height H is:

$$H = 8.2 \cdot Q^{\frac{1}{4}}$$

The theoretical curve correctly fits the experimental data except for the period of pyroclastic activity when the reduced height of the eruption column leads to underestimating the actual discharge rate. Soon after the pyroclastic flows the eruption increases again and the “experimental” data of discharge rate come back to values comparable to the theoretical ones.

In Fig. 4 we show a comparison between theoretical and experimental data together with seismicity accompanying the eruptive process. The occurrence of deep volcano tectonic

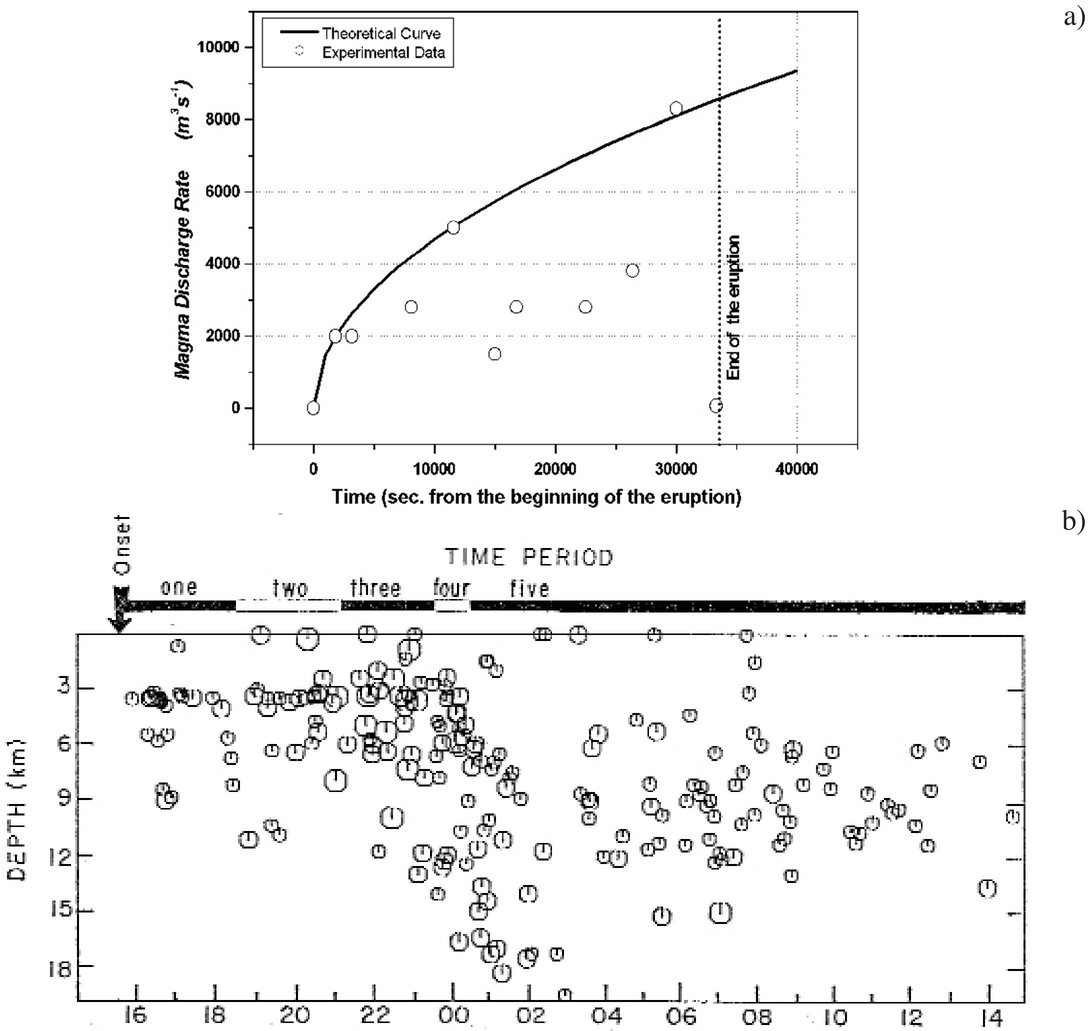

Fig. 4 - a) Simulation of the May 18, 1980 eruption at Mt. St. Helens, theoretical and experimental discharge rate; b) seismicity accompanying the eruption (scale along bottom of figure is U.T.C. hours; time period indicated is from May 18, 1980, 08:00 a.m. to May 19, 1980, 06:00 a.m.).

seismicity (10-15 km) beneath the volcano during the final stages of the eruption suggests that the whole eruptive process probably ends by a collapse of the magma chamber sealing the system and restoring the initial pressure conditions.

6. Conclusions

This paper highlights the role played by the magma chamber geometry on the temporal evolution of large explosive volcanic eruptions. A major conclusion is that shallow chambers of a large cross-sectional area tend to erupt with a higher rate than deep reservoirs of a small cross-sectional area during a fixed period of time.

We simulated the May 18, 1980 eruption at Mt. St. Helens (Washington, U.S.A.) and obtained a good fit of the experimental data; in particular, the theoretical temporal increase of the discharge rate matches well with the evolution of the phenomenon. We, moreover, predict the duration of the eruption, its ending, and the peak values of the discharge rate.

Our model investigates the influence of geometrical and physical parameters of the magma chambers on the temporal evolution of an explosive eruption; as a first order approximation, we consider the reservoir connected to the surface through a narrow conduit of variable geometry according to the eruptive flow characteristics. In our opinion, coupling the present model with a non-stationary model of conduit flow would provide a useful mean to further understand the transition between the Plinian phase and the pyroclastic flow emplacement.

Acknowledgments. Giuseppe De Natale and Giancarlo Neri made thoughtful reviews of this paper; their comments and suggestions resulted in a substantial improvement of the paper. This work was supported by the Gruppo Nazionale per la Vulcanologia.

References

Bower S.M. and Woods A.W.; 1997: *The control of magma volatile content and chamber depth on the mass erupted during explosive volcanic eruptions*. J. Geophys. Res. **102**, 10 273-10 290.

Carey S., Sigurdsson H., Gardner J.E. and Criswell W.; 1990: *Variation in column height and magma discharge rate-during the May 18, 1980 eruption of Mt. St. Helens*. J. Volcanol. Geotherm. Res. **86**, 67-78.

Christiansen R.L. and Peterson D.W.; 1981: *Chronology of the 1980 eruptive activity*. In: Lipman P.W. and Mullineaux D.R. (eds), The 1980 eruption of Mt. St. Helens. U.S.G.S. Prof. Pap. **1250**, U.S.G.S. Press, Seattle, pp. 17-67.

Folch A. and Martì J.; 1998: *A numerical model for temporal variations during explosive central vent eruptions*. J. Geophys. Res. **103**, 20 883-20 899.

Harris D.M., Rose Jr W.I., Roe R. and Thompson M.R.; 1981: *Radar observations of ash eruptions*. In: Lipman P.W. and Mullineaux D.R. (eds), The 1980 eruption of Mt. St. Helens, U.S.G.S. Prof. Pap. **1250**, U.S.G.S. Press, Seattle, pp. 323-334.

Lipman P.W. and Mullineaux D.R. (eds); 1981: *The 1980 eruption of Mount St. Helens*. U.S.G.S. Professional Papers **1250**, U.S.G.S. Press, Seattle.

Navon O. and Lyakhovsky V.; 1998: *Vesiculation processes in silicic magmas*. The physics of explosive eruptions. Geological society, London. Special Publications 27-50.

Scandone R.; 1996: *Factors controlling the temporal evolution of explosive eruptions*. J. Volcanol. Geotherm. Res. **72**, 71-83.

Scandone R. and Giacomelli L.; 2001: *The slow boling of magma chambers and the dynamics of explosive eruptions*. J. Volcanol. Geotherm. Res., **110**, 121-136.

Vergniolle S.; 1996: *Bubble size distribution in magma chambers and dynamics of basaltic eruptions*. E.P.S.L., **92**, 107-123.

Wilson L., Sparks R. S. J. and Walker G. P. L.; 1980: *Explosive volcanic eruptions: IV. The control of magma properties and conduit geometry on the eruption column behaviour*. Geophys. J. R. Astron. Soc., **63**, 117-148.

Woods A. W.; 1995: *The dynamics of explosive volcanic eruptions*. Rev. Geophys., **33**, 495-530.